



Cite this: *Nanoscale*, 2017, **9**, 4007

Negative Poisson's ratio in graphene oxide

Jing Wan,^a Jin-Wu Jiang*^a and Harold S. Park^b

We perform molecular dynamics simulations to investigate the Poisson's ratio of graphene oxide. We find that the Poisson's ratio can be effectively tuned by increasing the degree of oxidation of graphene oxide. More specifically, the Poisson's ratio decreases linearly from positive to negative with increasing oxidation, turning negative at room temperature for a degree of oxidation of 0.27, and reaching a value of -0.567 for fully oxidized graphene. The oxidation dependence of the Poisson's ratio is attributed to the tension-induced suppression of the ripples resulting from the oxidation, whose amplitude increases with increasing oxidation. Finally, we also demonstrate the temperature dependence of the Poisson's ratio in the graphene oxide.

Received 5th November 2016,

Accepted 17th February 2017

DOI: 10.1039/c6nr08657h

rsc.li/nanoscale

1. Introduction

The Poisson's ratio is the ratio of the resultant lateral strain to applied longitudinal strain. Most materials will contract in the lateral direction when they are stretched, resulting in a positive value for the Poisson's ratio. However, the Poisson's ratio is allowed to have a negative value within the classical elastic theory. For instance, the Poisson's ratio is limited to the range of $-1 < \nu < 0.5$ for isotropic three-dimensional materials.¹

Negative Poisson's ratios (NPRs) are desirable properties for bulk materials, because they enable unique behaviors such as enhanced sound and vibration absorption,² enhanced indentation resistance,³ enhanced toughness,⁴ and increased plane strain fracture resistance and increased shear modulus.⁵ Due to the significant interest in finding materials with these unique properties, many researchers have illustrated that various materials do exhibit NPR, including in crystalline SiO₂,⁶ cubic metals,⁷ ceramics,⁸ *etc.*, where the intrinsic NPR may emerge from a combination of the atomic structure and the type of bonding for a given material.^{7,9} Besides intrinsic NPR, NPR can be achieved through specific engineering of the structure, for example in permanent compressed metal foam,¹⁰ cellular structures,^{11,12} hinged frameworks,¹³ origami structures,^{14,15} and low porosity metallic periodic structures.¹⁶

While most NPR research has focused on bulk materials and structures, the field of NPR in nanomaterials has begun to emerge in recent years.¹⁷ Hall *et al.* found that the in-plane Poisson's ratio of carbon nanotube sheets (buckypaper) can be

tuned from positive to negative by mixing single-walled with multi-walled nanotubes.¹⁸ Yao *et al.* found that NPR might be possible in single-walled carbon nanotubes by substantial modifications of some structural parameters of bonding strength using the valence force field model.¹⁹ The Poisson's ratio for metal nanoplates can be made negative by a surface stress-induced phase transformation.²⁰ NPR was found to be intrinsic in single-layer black phosphorus due to its puckered configuration.^{21–23} NPR was also predicted to be intrinsic for few-layer orthorhombic arsenic using first-principles calculations.²⁴

As one of the most widely studied low-dimensional nanomaterials, graphene has also been found to exhibit NPR. The intrinsic NPR for single-layer graphene is a nonlinear phenomenon occurring at tensile strains larger than 6%.²⁵ The Poisson's ratio in graphene can also be changed into a negative value by some specific patterning. For instance, it has been shown that randomly oriented cuts,²⁶ periodic voids,²⁷ and pre-designed graphene kirigami²⁸ (kirigami ('kiru' cut; 'ori' fold; 'kami' paper) is the art of folding and cutting paper into beautiful and complex structures; the phrase 'graphene kirigami' indicates the application of this idea to graphene^{29,30}) will cause NPR for graphene. Meanwhile, out-of-plane rippling is another important mechanism to induce NPR for graphene, as the ripples will be flattened out during the in-plane stretching of graphene. It was found that the Poisson's ratio for graphene can be driven into the negative regime by thermally induced ripples at high temperatures above 1700 K,³¹ or vacancy-induced ripples,³² or compressive edge stress-induced ripples,³³ or hydrogenation-induced ripples.³⁴

Graphene oxide (GO) is an important chemically functionalized derivative of graphene. Specifically, GO membranes have shown great potential in many applications such as transparent conductors,^{35,36} chemical sensors,³⁷ capacitors,³⁸ polymer

^aShanghai Institute of Applied Mathematics and Mechanics, Shanghai Key Laboratory of Mechanics in Energy Engineering, Shanghai University, Shanghai 200072, People's Republic of China. E-mail: jwjiang5918@hotmail.com
^bDepartment of Mechanical Engineering, Boston University, Boston, Massachusetts 02215, USA

composites,³⁹ batteries,⁴⁰ biosensors,⁴¹ water desalination and purification.^{42,43} For more details on the application of GO, readers are referred to some comprehensive reviews, *e.g.* ref. 37, 44 and 45.

Several experiments have observed substantial rippling in the GO,^{46,47} which can affect its mechanical properties.⁴⁸ In particular, these ripples in GO reduce the Young's modulus of GO papers up to 60%.⁴⁷ According to the above studies on the ripple-induced NPR in graphene, the ripples in GO should strongly impact its Poisson's ratio, and may even induce a NPR in GO. Furthermore, the degree of oxidation is an important factor for the tuning of many physical or mechanical properties in GO,^{49–51} including the insulator–semiconductor–semimetal transition⁵² and the electrical conductivity.⁵³ Hence, it is of practical importance to examine the possible NPR in the GO and investigate the dependence of the Poisson's ratio on the degree of oxidation in the GO, which comprise the focus of the present study. In this paper, in order to quantify the oxidized area in GO, the degree of oxidation (p) is defined as the ratio of the number of the oxidized carbon atoms to the total number of carbon atoms. In experiments, it is observed that the degree of oxidation in GO can exceed 80%.⁵⁴

In this paper, we calculate the Poisson's ratio of GO with different degrees of oxidation, and focus on identifying the relationship between the Poisson's ratio and the degree of oxidation. We find that the Poisson's ratio decreases linearly from positive to negative with the increase of the degree of oxidation in the range $p \in [0, 1.0]$, where the most negative value for the Poisson's ratio is -0.567 for fully oxidized graphene (*i.e.*, $p = 1.0$). The underlying mechanism for the reduction of the Poisson's ratio is the suppression of the oxidation-induced ripples during the stretching of the GO. The temperature effect on the Poisson's ratio is also studied for GO of various degrees of oxidation.

II. Structure and simulation details

Fig. 1 shows the structure for GO of dimension 20×20 nm. The epoxy and hydroxyl groups (of ratio 2:3) are distributed

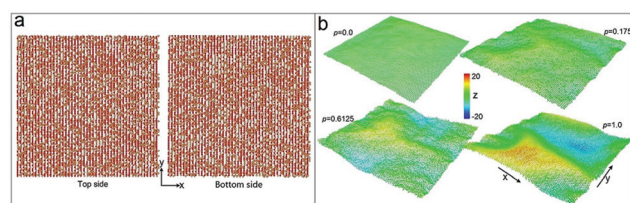


Fig. 1 Structure for graphene oxide of size 20×20 nm at room temperature. (a) The configuration of the functional groups on the fully oxidized graphene. The left panel is the view of groups above graphene. The right panel is the view of groups below graphene. The red color atom is the oxygen atom, and the yellow color atom is the hydrogen atom. (b) The left top panel shows pure graphene (*i.e.*, the degree of oxidation, $p = 0$). The other three panels show graphene oxide with $p = 0.175$, 0.6125 , and 1.0 , respectively. The color bar is with respect to the z -coordinate of each atom.

onto both sides of graphene, which can result in structures with lower energy.^{55,56} More specifically, in the fully oxidized graphene, *i.e.*, the degree of oxidation $p = 1$, the epoxy groups are first distributed onto both sides of graphene randomly, followed by the addition of hydroxyl groups in an alternating manner as shown in Fig. 1(a).⁵⁷ This alternating distribution can result in a structure with lower energy.⁵⁶ Fig. 1(a) shows the resultant configuration for the fully oxidized graphene, *i.e.*, with a degree of oxidation $p = 1$. The side view clearly shows that the functional groups are uniform on both sides of the graphene sheet. The top view shows that the functional groups are uniform in the plane of the graphene sheet, *i.e.* the x - y plane.

In the resultant configuration, the oxygen atoms in the hydroxyl group are on top of the carbon atom with a distance of 1.5 \AA , and the position of the hydrogen atoms are at 1.0 \AA above the oxygen atoms. Epoxide oxygens are on top of the middle of carbon–carbon bonds with a distance of 1.3 \AA . The degrees of oxidation are $p = 0, 0.175, 0.6125$ and 1.0 for these four configurations shown in Fig. 1(b), all shown at room temperature. For a given degree of oxidation p , the structure is obtained by randomly removing $(1 - p)$ groups from the fully oxidized graphene, so that the structures of different degrees of oxidation are comparable.

Due to the functionalization of graphene, clear evidence of oxidation-induced rippling in the GO can be observed as shown in Fig. 1. The height of the ripples in the z -direction increases with increasing degree of oxidation, which will be quantified in the next section. We note the existence of thermally-induced ripples in the pure graphene ($p = 0$), the heights of which are considerably smaller than the oxidation-induced ripples. Furthermore, there are obvious regional differences in the z -coordinates in the fully oxidized graphene. The configuration of the fully oxidized graphene ($p = 1.0$) shown in Fig. 1(b) appears similar to the first vibrational mode of the graphene oxide, where periodic boundaries have been applied in both x and y directions. It is because the first vibration mode has the lowest frequency, so it will make a predominant contribution to most thermally-related quantities.^{58,59} Our results indicate that the functional groups may assist the excitation of the first vibrational mode.

To determine the Poisson's ratio, we applied tensile mechanical strain along the x (armchair)-direction, while the structure was allowed to fully relax in the y (zigzag)-direction using molecular dynamics (MD) simulations. Periodic boundary conditions were also applied in the y -direction, while both ends in the x -direction were translated rigidly to apply the tensile deformation to the GO. The standard Newton equations of motion are integrated in time using the velocity Verlet algorithm with a time step of 1 fs . In this work, the MD simulations were performed using the Sandia-developed open source code LAMMPS.⁶⁰

The optimized potentials for liquid simulations-all atoms (OPLS-AA) force field is used to describe the interaction between functional groups and graphene.⁶¹ This force field has previously been used successfully to simulate graphene

oxide.^{62,63} The harmonic interactions are used to describe both bond stretching and angle bending. Dihedral interactions are described by the OPLS potential.^{64,65} van der Waals interactions between atoms are described by using a 12-6 Lennard-Jones (LJ) potential. The parameters of the LJ potential for the O–O interaction are $\epsilon_{\text{O-O}} = 0.1553 \text{ kcal mol}^{-1}$ and $\sigma_{\text{O-O}} = 3.166 \text{ \AA}$.⁶⁶ For the C–C LJ potential, the parameters are $\epsilon_{\text{C-C}} = 0.0553 \text{ kcal mol}^{-1}$ and $\sigma_{\text{C-C}} = 3.4 \text{ \AA}$.⁶⁷ The LJ potential parameters for the C–O interaction are obtained following the Lorentz–Berthelot combining rules.⁶⁶

III. Results and discussion

We first show in Fig. 2 the resultant strain in the y -direction for a given applied strain in the x -direction for GO at room temperature. The Poisson's ratio is obtained as the slope of the curve in the small strain range $\epsilon_x \in [0, 0.01]$. The mechanical response, and also the Poisson's ratio, is clearly sensitive to the degree of oxidation. The obtained values for the Poisson's ratio are 0.234, 0.064, and -0.505 corresponding to the degrees of oxidation of 0, 0.175, and 0.875, respectively. As can be seen, the Poisson's ratio becomes negative between oxidation degrees of 0.175 and 0.875. We show later that the exact degree of oxidation at which the Poisson's ratio becomes negative at room temperature is about 0.27.

To understand the NPR in the GO with a high degree of oxidation, we point out that the GO shown in Fig. 1 looks similar to a wrinkled paper sheet. It is well known that a highly wrinkled paper sheet will exhibit a significant NPR due to the suppression of the ripples during the stretching process.^{32,68} This behavior was attributed to the disorder-related auxetic egg-rack mechanism, rather than the intrinsic properties of the paper itself.⁶⁹ It is thus possible that the NPR of the GO is induced by the oxidation-induced ripples.

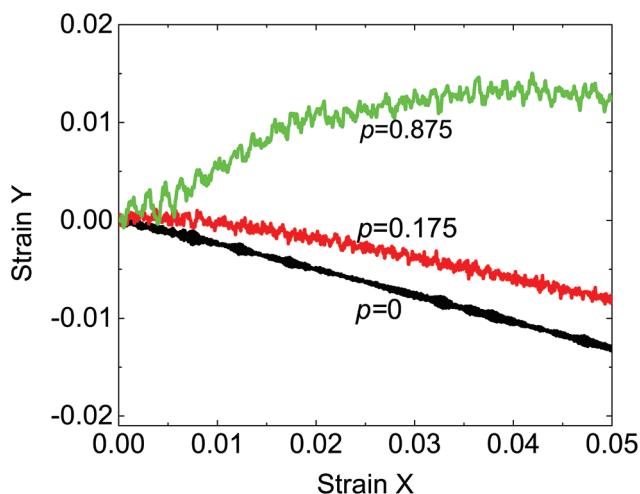


Fig. 2 The resultant strain in the lateral direction *versus* the applied strain along the longitudinal direction at room temperature during the stretching of the graphene oxide with degrees of oxidation $p = 0, 0.175,$ and 0.875 .

To verify the oxidation-induced ripple effect on the NPR in GO, we present some snapshots in Fig. 3 for the configuration of GO with a degree of oxidation $p = 0.6125$ during the stretching process, where the figure color bars indicate the atomic coordinates in the z -direction. As can be seen, the rippling amplitude decreases markedly with increased tensile deformation, which implies flattening of the initial oxidation-induced ripples. To provide a more quantitative description for this flattening of the ripple, we simplify the configuration of the ripple by a three-dimensional tetrahedron structure shown in Fig. 4(a). The dihedral angle for the tetrahedron reflects the amplitude of the ripple. Fig. 4(b) shows that the dihedral angle decreases during the stretching of the GO, which results in the expansion of the structure in the y -direction, indicating a NPR phenomenon. It should be noted that these out-of-plane ripples in GO can induce in-plane NPR during the in-plane stretching, but the Poisson's ratio is positive in the out-of-plane direction.

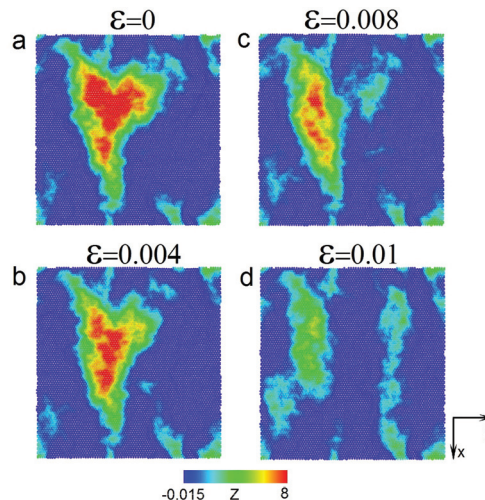


Fig. 3 Structural evolution of the ripples in the graphene oxide with a degree of oxidation $p = 0.6125$ during stretching. The color bar is with respect to the z -coordinate of each carbon atom.

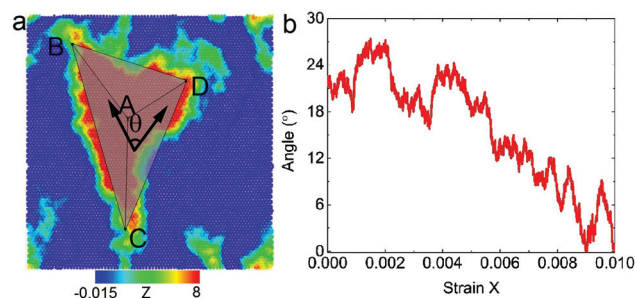


Fig. 4 A simplified geometrical model for the ripple. (a) The ripple is represented by the tetrahedron ABCD. The dihedral angle between the planes ACB and ACD quantifies the amplitude of the ripple. (b) The dihedral angle *versus* the applied strain. The color bar corresponds to the z -coordinate of each carbon atom.

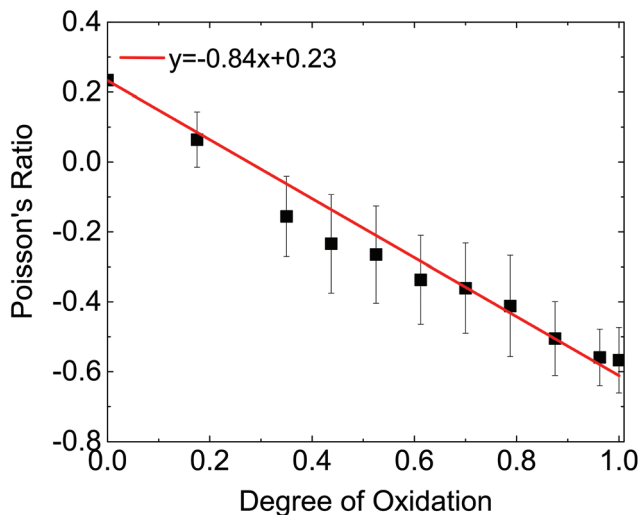


Fig. 5 The Poisson's ratio of graphene versus the degree of oxidation for graphene oxide at room temperature.

Fig. 5 shows the dependence of the Poisson's ratio on the degree of oxidation in the GO at room temperature. The Poisson's ratio decreases almost linearly with the increase of the degree of oxidation, which can be fitted to a linear function of $y = -0.84x + 0.23$. This also implies that the Poisson's ratio becomes negative for GO with the degree of oxidation above 0.27. The slope of -0.84 is close to the slope value of -0.77 for hydrogenated graphene.³⁴ We note that the degree of oxidation of GO can be controlled in experiments,^{50,70} and thus graphene oxide samples with different degrees of oxidation can be prepared. As recent experiments have demonstrated the ability to stretch graphene kirigami over a wide range of uniaxial strains,³⁰ we expect that it will also be possible to stretch graphene oxide. Based on these experiments, we believe it will be possible to experimentally stretch and measure the Poisson's ratio of graphene oxide in the near future.

To examine the dependence of the Poisson's ratio on the degree of oxidation, we calculate the amplitude of the ripples in the GO for different degrees of oxidation. We introduce the following standard deviation of out-of-plane displacement ($\langle h \rangle$) to describe the amplitude of the ripples,

$$\langle h \rangle = \sqrt{\sum_{i=1,N} (h_i - h_{av})^2 / N}, \quad (1)$$

where h_{av} is the average of all carbon atoms in the z -direction. Fig. 6 shows that the standard deviation for the out-of-plane displacements increases monotonically with increasing degree of oxidation, which can be fitted to the linear function $y = 5.3x + 1.0$. This means that the overall amplitude for the oxidation-induced ripples is larger in GO with a higher degree of oxidation, which will lead to smaller Poisson's ratio as the ripples have a negative effect on the Poisson's ratio according to Fig. 4.

The rippling of thin sheets is known to lead to NPR,⁶⁸ and has been shown to lead to NPR in graphene. An interesting

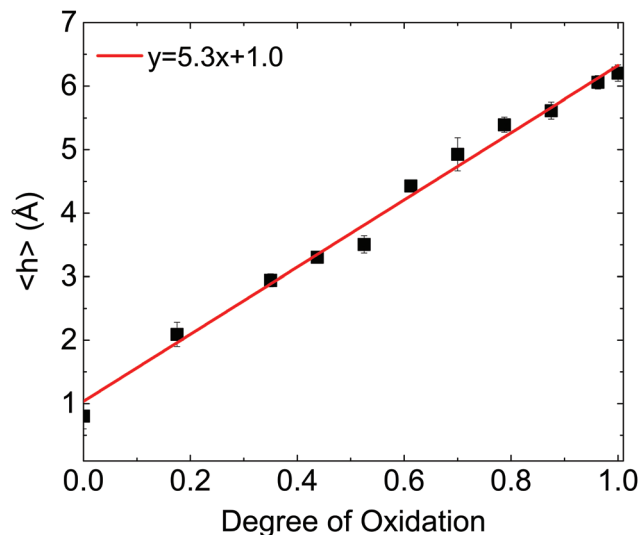


Fig. 6 The mean out-of-plane displacement amplitude of carbon atoms versus the degree of oxidation. h_i is the position of the i th atom, and h_{av} is the averaged position of all carbon atoms in the z -direction. N is the total atom number.

finding in the present study is that the ripple amplitude increases monotonically with the increase of the degree of oxidation, which leads to the monotonic decrease of the Poisson's ratio as shown in Fig. 5. This is different from the hydrogenation effect on the Poisson's ratio of graphene, in which the Poisson's ratio decreases in the small hydrogenation percentage range but increases for larger hydrogenation percentages.³⁴ This is because the fully hydrogenated graphene becomes a crystal structure, so the amplitude of the hydrogenation-induced ripples will decrease for highly hydrogenated graphene. However, there is no crystal structure formation in fully oxidized graphene due to the randomness in the distribution of the functional groups.^{54,57} Furthermore, several experiments have demonstrated that other physical properties in graphene oxide, including structural and electrochemical properties, also change monotonically with the increase of the degree of oxidation in the range ($0.3 < p < 0.8$).^{50,53}

It should be noted that the substantial regional difference of the Z -coordinate in GO is due to the oxidation-induced changes in the interaction between carbon atoms. More specifically, the chemical doping of the epoxy and hydroxyl groups leads to the sp^2 - sp^3 hybridization of carbon atoms. This chemical doping greatly changes the initial equilibrium force field parameters (bond length, bond angle and dihedral angles) of carbon atoms. As a result, the carbon atoms in graphene will change their positions in the out-of-plane direction, as required by the new equilibrium force field parameters. That is the origin for the increase of the out-of-plane displacement amplitude of carbon atoms with increasing degree of oxidation.

As a result of the thermal vibrations, there are some thermally-induced ripples in pure graphene. These thermally-induced ripples (in the left top panel of Fig. 1(b)) are much

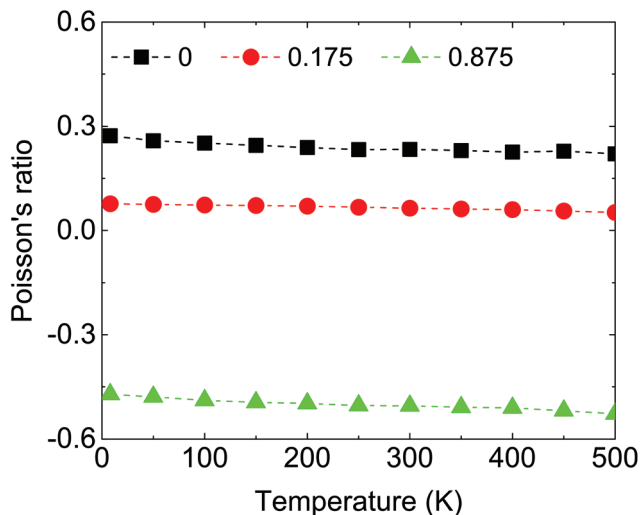


Fig. 7 The temperature dependence of the Poisson's ratio of the GO with degrees of oxidation $p = 0, 0.175,$ and 0.875 .

smaller than the oxidation-induced ripples (other panels shown in Fig. 1(b)). In pure graphene the temperature must be exceptionally high, *i.e.* around 2000 K, in order to obtain a negative Poisson's ratio.³¹ Thus, the temperature effect is not as strong as the oxidation effect. Although the thermally-induced ripples are much smaller than the oxidation-induced ripples in the GO, the thermally-induced ripples may have a strong effect on the Poisson's ratio of GO at high temperatures. We present in Fig. 7 the temperature dependence of the Poisson's ratio of the GO with three different degrees of oxidation, *i.e.*, $p = 0, 0.175,$ and 0.875 . The temperature-induced reduction of the Poisson's ratio is less than 0.06 for temperature increasing from 8 K to 500 K. As can be seen, compared with the changes in the Poisson's ratio due to oxidation, the changes in the Poisson's ratio due to temperature for GO are much smaller. We note that the value of the Poisson's ratio for the pure graphene is 0.28 at 8 K as shown in Fig. 7, which is quite close to the previous value of 0.3 obtained from the Brenner potential.²⁵

IV. Conclusion

In summary, we have calculated the Poisson's ratio of graphene oxide using classical molecular dynamics simulations. We find that the Poisson's ratio is sensitive to the degree of oxidation; it decreases from positive to negative with an increase of the degree of oxidation. The oxidation-induced reduction of the Poisson's ratio is attributed to the flattening of the oxidation-induced ripples in the GO, whose amplitude increases with increasing GO oxidation. The largest negative Poisson's ratio we find is -0.567 when graphene is fully oxidized.

Acknowledgements

The work is supported by the Recruitment Program of Global Youth Experts of China, the National Natural Science

Foundation of China (NSFC) under Grant No. 11504225 and the start-up funding from Shanghai University. HSP acknowledges the support of the Mechanical Engineering department at Boston University.

References

- 1 L. D. Landau and E. M. Lifshitz, *Theory of Elasticity*, Pergamon, Oxford, 1995.
- 2 A. W. Lipsett and A. I. Beltzer, *J. Acoust. Soc. Am.*, 1988, **84**, 2179.
- 3 R. Lakes and K. Elms, *J. Compos. Mater.*, 1993, **27**, 1193.
- 4 J. Choi and R. Lakes, *Int. J. Fract.*, 1996, **80**, 73.
- 5 X. Huang and S. Blackburn, *Key Eng. Mater.*, 2002, **206**, 201.
- 6 N. R. Keskar and J. R. Chelikowsky, *Nature*, 1992, **358**, 222.
- 7 R. H. Baughman, J. M. Shacklette, A. A. Zakhidov and S. Stafstrom, *Nature*, 1998, **392**, 362.
- 8 F. Song, J. Zhou, X. Xu, Y. Xu and Y. Bai, *Phys. Rev. Lett.*, 2008, **100**, 245502.
- 9 A. Alderson and K. E. Evans, *Phys. Rev. Lett.*, 2002, **89**, 225503.
- 10 R. S. Lakes, *Science*, 1987, **235**, 1038.
- 11 J. B. Choi and R. S. Lakes, *J. Mater. Sci.*, 1992, **27**, 4678.
- 12 J. B. Choi and R. S. Lakes, *J. Mater. Sci.*, 1992, **27**, 5375.
- 13 R. Lakes, *Nature*, 1993, **361**, 511.
- 14 M. Schenk and S. D. Guest, *Proc. Natl. Acad. Sci. U. S. A.*, 2013, **110**, 3276.
- 15 Z. Y. Wei, Z. V. Guo, L. Dudte, H. Y. Liang and L. Mahadevan, *Phys. Rev. Lett.*, 2013, **110**, 215501.
- 16 M. Taylor, L. Francesconi, M. Gerendas, A. Shanian, C. Carson and K. Bertoldi, *Adv. Mater.*, 2014, **26**, 2365.
- 17 J.-W. Jiang, S. Y. Kim and H. S. Park, *Appl. Phys. Rev.*, 2016, **3**, 041101.
- 18 L. J. Hall, V. R. Coluci, D. S. Galvão, M. E. Kozlov, M. Zhang, S. O. Dantas and R. H. Baughman, *Science*, 2008, **320**, 504.
- 19 Y. T. Yao, A. Alderson and K. L. Alderson, *Phys. Status Solidi B*, 2008, **245**, 2373.
- 20 D. T. Ho, S.-D. Park, S.-Y. Kwon, K. Park and S. Y. Kim, *Nat. Commun.*, 2014, **5**, 3255.
- 21 J.-W. Jiang and H. S. Park, *Nat. Commun.*, 2014, **5**, 4727.
- 22 M. Elahi, K. Khaliji, S. M. Tabatabaei, M. Pourfath and R. Asgari, *Phys. Rev. B: Condens. Matter*, 2015, **91**, 115412.
- 23 G. Qin, Q.-B. Yan, Z. Qin, S.-Y. Yue, H.-J. Cui, Q.-R. Zheng and G. Su, *Sci. Rep.*, 2016, **6**, 21233.
- 24 J. Han, J. Xie, Z. Zhang, D. Yang, M. Si and D. Xue, *Appl. Phys. Express*, 2015, **8**, 041801.
- 25 J.-W. Jiang, T. Chang, X. Guo and H. S. Park, *Nano Lett.*, 2016, **16**, 5286.
- 26 J. N. Grima, L. Mizzi, K. M. Azzopardi and R. Gatt, *Adv. Mater.*, 2016, **28**, 385.
- 27 V. H. Ho, D. T. Ho, S.-Y. Kwon and S. Y. Kim, *Phys. Status Solidi B*, 2016, **253**, 1303.
- 28 K. Cai, J. Luo, Y. Ling, J. Wan and Q.-h. Qin, *Sci. Rep.*, 2016, **6**, 35157.

- 29 Z. Qi, D. K. Campbell and H. S. Park, *Phys. Rev. B: Condens. Matter*, 2014, **90**, 245437.
- 30 M. K. Blees, A. W. Barnard, P. A. Rose, S. P. Roberts, K. L. McGill, P. Y. Huang, A. R. Ruyack, J. W. Kevek, B. Kobrin, D. A. Muller and P. L. McEuen, *Nature*, 2015, **524**, 204.
- 31 K. V. Zakharchenko, M. I. Katsnelson and A. Fasolino, *Phys. Rev. Lett.*, 2009, **102**, 046808.
- 32 J. N. Grima, S. Winczewski, L. Mizzi, M. C. Grech, R. Cauchi, R. Gatt, D. Attard, K. W. Wojciechowski and J. Rybicki, *Adv. Mater.*, 2015, **27**, 1455.
- 33 J.-W. Jiang and H. S. Park, *Nano Lett.*, 2016, **16**, 2657.
- 34 J.-W. Jiang, T. Chang and X. Guo, *Nanoscale*, 2016, **8**, 15948.
- 35 O. C. Compton and S. T. Nguyen, *Small*, 2010, **6**, 711.
- 36 S. Wu, Z. Yin, Q. He, X. Huang, X. Zhou and H. Zhang, *J. Phys. Chem. C*, 2010, **114**, 11816.
- 37 X. Huang, Z. Yin, S. Wu, X. Qi, Q. He, Q. Zhang, Q. Yan, F. Boey and H. Zhang, *Small*, 2011, **7**, 1876.
- 38 H. Wang, Y. Yang, Y. Liang, J. T. Robinson, Y. Li, A. Jackson, Y. Cui and H. Dai, *Nano Lett.*, 2011, **11**, 2644.
- 39 R. Sengupta, M. Bhattacharya, S. Bandyopadhyay and A. K. Bhowmick, *Prog. Polym. Sci.*, 2011, **36**, 638.
- 40 F. Yao, F. Gunes, H. Q. Ta, S. M. Lee, S. J. Chae, K. Y. Sheem, C. S. Cojocar, S. S. Xie and Y. H. Lee, *J. Am. Chem. Soc.*, 2012, **134**, 8646.
- 41 Y. Liu, X. Dong and P. Chen, *Chem. Soc. Rev.*, 2012, **41**, 2283.
- 42 S. P. Surwade, S. N. Smirnov, I. V. Vlassiuk, R. R. Unocic, G. M. Veith, S. Dai and S. M. Mahurin, *Nat. Nanotechnol.*, 2015, **10**, 459.
- 43 L.-C. Lin and J. C. Grossman, *Nat. Commun.*, 2015, **6**, 8335.
- 44 M. J. Allen, V. C. Tung and R. B. Kaner, *Chem. Rev.*, 2010, **10**, 132.
- 45 K. P. Loh, Q. Bao, G. Eda and M. Chhowalla, *Nat. Chem.*, 2010, **2**, 1015.
- 46 T. Szabó, O. Berkesi, P. Forgó, K. Josepovits, Y. Sanakis, D. Petridis and I. Dékány, *Chem. Mater.*, 2006, **18**, 2740.
- 47 X. Shen, X. Lin, N. Yousefi, J. Jia and J.-K. Kim, *Carbon*, 2014, **66**, 84.
- 48 L. J. Cote, J. Kim, Z. Zhang, C. Sun and J. Huang, *Soft Matter*, 2010, **6**, 6096.
- 49 G. Eda and M. Chhowalla, *Adv. Mater.*, 2010, **22**, 2392.
- 50 K. Krishnamoorthy, M. Veerapandian, K. Yun and S.-J. Kim, *Carbon*, 2013, **53**, 38.
- 51 W. Li, J. Liu and C. Yan, *Carbon*, 2013, **55**, 313.
- 52 G. Eda, C. Mattevi, H. Yamaguchi, H. Kim and M. Chhowalla, *J. Phys. Chem. C*, 2009, **113**, 15768.
- 53 O. C. Compton, B. Jain, D. A. Dikin, A. Abouimrane, K. Amine and S. T. Nguyen, *ACS Nano*, 2011, **5**, 4380.
- 54 K. Erickson, R. Erni, Z. Lee, N. Alem, W. Gannett and A. Zettl, *Adv. Mater.*, 2010, **22**, 4467.
- 55 A. Bagri, C. Mattevi, M. Acik, Y. J. Chabal, M. Chhowalla and V. B. Shenoy, *Nat. Chem.*, 2010, **2**, 581.
- 56 N. Ghaderi and M. Peressi, *J. Phys. Chem. C*, 2010, **114**, 21625.
- 57 J. T. Paci, T. Belytschko and G. C. Schatz, *J. Phys. Chem. C*, 2007, **111**, 18099.
- 58 A. Krishnan, E. Dujardin, T. W. Ebbesen, P. N. Yianilos and M. M. J. Treacy, *Phys. Rev. B: Condens. Matter*, 1998, **58**, 14013.
- 59 J.-W. Jiang, J.-S. Wang and B. Li, *Phys. Rev. B: Condens. Matter*, 2009, **80**, 113405.
- 60 S. J. Plimpton, *J. Comput. Phys.*, 1995, **117**, 1.
- 61 W. L. Jorgensen, D. S. Maxwell and J. Tirado-Rives, *J. Am. Chem. Soc.*, 1996, **118**, 11225.
- 62 C.-J. Shih, S. Lin, R. Sharma, M. S. Strano and D. Blankschtein, *Langmuir*, 2011, **28**, 235.
- 63 W. Zhao, Y. Wang, Z. Wu, W. Wang, K. Bi, Z. Liang, J. Yang, Y. Chen, Z. Xu and Z. Ni, *Sci. Rep.*, 2015, **5**, 11962.
- 64 J. Chen, X. Wang, C. Dai, S. Chen and Y. Tu, *Physica E*, 2014, **62**, 59.
- 65 N. R. Tummala and A. Striolo, *J. Phys. Chem. B*, 2008, **112**, 1987.
- 66 R. Nair, H. Wu, P. Jayaram, I. Grigorieva and A. Geim, *Science*, 2012, **335**, 442.
- 67 A. Cheng and W. Steele, *J. Chem. Phys.*, 1990, **92**, 3858.
- 68 D. H. Boal, U. Seifert and J. C. Shillcock, *Phys. Rev. E: Stat. Phys., Plasmas, Fluids, Relat. Interdiscip. Top.*, 1993, **48**, 4274.
- 69 J. N. Grima, J. J. Williams and K. E. Evans, *Chem. Commun.*, 2005, 4065.
- 70 G. Wang, X. Sun, C. Liu and J. Lian, *Appl. Phys. Lett.*, 2011, **99**, 053114.